Proceedings of ICTACEM 2014
International Conference on Theoretical, Applied, Computational and Experimental Mechanics
December 29-31, 2014, IIT Kharagpur, India
ICTACEM-2014/394

Advantages of a deterministic thermostat utilizing the entire phase space over other thermostatting techniques

Puneet Kumar Patra[a] and Baidurya Bhattacharya[b1]
[a] Advanced Technology Development Center, Indian Institute of Technology Kharagpur, Kharagpur, India 721302
[b] Dept. of Civil Engineering, Indian Institute of Technology Kharagpur, Kharagpur, India 721302

ABSTRACT

In this work, we highlight the relative advantages of using a deterministic thermostat that utilizes the entire phase-space (PB) over other thermostats that use either the configurational (BT) or the kinetic (NH) space for temperature control. The efficacy of PB thermostat is demonstrated using a simple model of thermal conduction comprising of Lennard-Jones particles. Out of the three thermostats, only the PB dynamics generates a consistent temperature profile for (i) different system size, and (ii) large temperature difference between the hot and the cold thermostats. The difference in temperature profiles occurs due to the thermostat-dependent dynamical properties of the thermostatted system. We corroborate this finding by calculating the radial distribution functions (RDFs) due to the three thermostats. Our results indicate that, for nonequilibrium cases, with the increasing strength of nonlinearity (temperature difference), the disparity between the RDFs increases. We also show that only in equilibrium, all the three thermostats result in identical RDFs. With RDFs bearing a direct relationship to several thermodynamic variables, a different RDF implies a different macroscopic property of the system. Consequently, it becomes of utmost importance to select a proper thermostat for obtaining statistical-mechanical properties from thermostatted molecular dynamics simulations.

Keywords: Molecular Dynamics Simulation, Thermostat, Nosé-Hoover, Configurational temperature

1. INTRODUCTION

Thermostats in molecular dynamics simulations enable us to perform "numerical experiments" that have close resemblance to the "real life experiments" performed at constant temperature. These constant temperature (global and local) molecular dynamics has been used to calculate important transport properties like thermal conductivity [1, 2], diffusion constant [3, 4], viscosity [5] etc. for several systems. In general, a thermostatting algorithm works by withdrawing the excess heat from the system and therefore, are a must for simulating a driven nonequilibrium system, providing stability to these simulated processes. Temperature control can be done through velocity constraining [6-8], stochastic [9-11] or deterministic [4, 12-19] algorithms. Amongst the three, the deterministic ones are the most appealing for being autonomous, time reversible and physics preserving [20], despite the issues of nonergodicity associated with most

[1] Further author information: (Send correspondence to B.B)
B.B.: E-mail: baidurya@ iitkgp.ac.in, Telephone: +91 (3222) 28-3422, Address: Department of Civil Engineering, Indian Institute of Technology Kharagpur, West Bengal 721302, India

of them [21-25]. Regardless of the temperature being controlled, every deterministic thermostat generates a dynamics consistent with Gibbs distribution in equilibrium,

$$f(\mathbf{x},\mathbf{p}) = \frac{1}{Z}\exp\left[-\beta H(\mathbf{x},\mathbf{p})\right], \tag{1}$$

where, **x** and **p** represent the position and the velocity of the particles, respectively. H(**x,p**) is the energy of the system, $\beta = (k_B T)^{-1}$ and Z represents the partition function. The ability of different thermostats to provide equivalent results in equilibrium, despite controlling different measures of temperatures, occurs due to the equality of the kinetic, configurational and Rugh's temperature [26-28]. The general relationship of temperature with an arbitrary phase-space function (B) [28] can be expressed through (2).

$$\frac{1}{k_B T} = \frac{\langle \nabla . \nabla B \rangle}{\langle \nabla H . \nabla B \rangle} = \lim_{t\to\infty} \frac{1}{t}\int_0^t \left(\nabla . \frac{\nabla B}{\nabla H . \nabla B} \right) d\tau \tag{2}$$

In (2), ∇ represents the gradient operator carried with respect to all the phase space variables. Depending on functional form of B, different measures of temperature can be obtained: if B taken to be the total kinetic energy of the system, T represents the kinetic temperature, T_{KIN}, if B is taken to be the total potential energy of the system, T represents the configurational temperature, T_{CON}:

$$\begin{aligned} B = \sum_{i=1}^{3N} \frac{p_i^2}{2m} \quad &\rightarrow \quad T_{KIN} = \frac{2}{3Nk_B}\sum_{i=1}^{3N}\frac{p_i^2}{2m}; \\ B = \phi(r_i) \quad &\rightarrow \quad T_{CON} = \frac{1}{k_B}\frac{\|\nabla_r \phi\|^2}{\nabla_r{}^2 \phi}. \end{aligned} \tag{3}$$

The most common and well known thermostatting scheme, the Nosé-Hoover (NH) thermostat [12, 13], works by constraining T_{KIN}. However, controlling the kinetic part of temperature alone is not adequate for simulating some heat driven nonequilibrium molecular dynamics simulations [29, 30] like in presence of large gradients or simulations involving very long molecular systems (ex. polymers and proteins). The difficulties of kinetic temperature based temperature control get exemplified in flowing non-equilibrium systems as well where determining the spatial and time dependent streaming velocity is difficult. These problems can be alleviated with thermostats based on controlling the configurational temperature, for example the Braga-Travis (BT) configurational thermostat [31].

Importantly, $T = T_{KIN} = T_{CON}$ does not hold true for nonequilibrium cases, except in situations where the system exhibits local thermodynamic equilibrium (LTE). In fact, different thermostats result in different dynamical properties of the system [32]. Consequently, using a correct thermostatting method becomes a key step for obtaining results commensurate with real life experiments. Additionally, the thermostats, based on controlling either the kinetic or configurational part of the temperatures, are usually unable to generate a temperature profile consistent with the predictions of LTE [33] – the system is in equilibrium locally and hence, the configurational and kinetic temperatures must be equal locally. To overcome these issues, a new thermostat has been recently proposed (PB) that simultaneously controls the kinetic as well as configurational temperatures [19]. It has been argued that the PB thermostat is a better algorithm for nonequilibrium situations (like thermal conduction) because of its ability to generate consistent temperature profile.

In this work, we build upon the already known advantages of PB thermostat and show that it is able to provide better consistency in temperature control even when a large temperature gradient is imposed on the system as well as when the system size is increased. The results of PB thermostat are compared with the Nosé-Hoover (NH) kinetic thermostat and the Braga-Travis (BT) configurational thermostat. We also qualitatively analyse the difference in the dynamical properties due to the different thermostats by computing the radial distribution functions (RDFs). This paper is organized as following: in the next section we detail the three different thermostats, following which we look at simulation results for both equilibrium and nonequilibrium cases, and lastly, we summarize the findings.

2. THE DIFFERENT THERMOSTATS AND THERMAL CONDUCTION MODEL

Although, chronologically developed last, we begin with the PB thermostat [19], since one can modify its equations of motion to obtain the other well-known kinetic and configurational thermostats. The equations of motion of PB thermostat for a three dimensional system comprising of N particles constrained at a temperature T_0 are:

$$
\begin{aligned}
\dot{r}_i &= \frac{p_i}{m_i} - \xi \frac{\partial \phi}{\partial r_i} \\
\dot{p}_i &= -\frac{\partial \phi}{\partial r_i} - \eta\, p_i \\
\dot{\xi} &= \frac{1}{Q_\xi} \sum_{i=1}^{3N} \left(\left(\frac{\partial \phi}{\partial r_i} \right)^2 - k_B T_0 \frac{\partial^2 \phi}{\partial r_i^2} \right) \\
\dot{\eta} &= \frac{1}{Q_\eta} \sum_{i=1}^{3N} \left(\frac{p_i^2}{m_i} - k_B T_0 \right)
\end{aligned}
\tag{4}
$$

The terms Q_i denote the mass of the i^{th} reservoir variable. In (4) the variables ξ and η act on the generalized position and velocity of the particle to constrain the configurational and kinetic temperatures, respectively. The temperature of the system is fixed by making the time derivatives of these feedback variables dependent on the instantaneous difference between the desired temperature and the instantaneous temperature corresponding to feedback variable.

The easiest route to develop (4) is analogous to the derivation (the guessing method) first highlighted for NH thermostat by Hoover [34]. We begin by assuming that the coupling between the position and velocity variables is according to the first two sub-equations of (4). Next, the extended phase space Liouville's equation is solved keeping in mind that the dynamics must satisfy the extended canonical distribution function. The outcome of this procedure gives the time evolution of the thermostat variables - the last two sub-equations of (4). Under the given nature of coupling, (4) is the only solution that simultaneously satisfies the extended phase space Liouville's equation and generates a canonical distribution i.e. the solution is unique.

The thermostat variables fluctuate around a mean value (usually zero), implying that the long-time averaged value of the temporal evolution of thermostat variables is zero i.e. $\langle \dot{\xi} \rangle = \langle \dot{\eta} \rangle = 0$.

As a result, it is not very difficult to see that from the third equation of (4) results in control of T_{CON} (see (3)) while the fourth equation of (4) results in control of T_{KIN}. The PB thermostat satisfies the general temperature control algorithm for arbitrary coupling between the different variables. One can obtain the NH thermostat by setting $\xi = \dot{\xi} = 0$ in (4). The BT thermostat can be obtained by setting $\eta = \dot{\eta} = 0$ in (4).

For all the three thermostats chosen in this study, the rate of convergence to the canonical ensemble is dependent on the proper choice of thermostat mass factors [35, 36]. Since, the appropriate value of these masses is dependent on the problem being studied, a unified principle

for their selection is difficult to determine. We would also like to stress that all the three thermostats satisfy the extended Liouville's equation even if the coupling terms are augmented with a switching function in such a manner that only a small subdomain is thermostatted. This kind of a partial thermostatting is able to generate a canonical distribution as well. The utility of partial thermostatting is manifold – especially for situations that demand different regions to be thermostatted at different temperatures.

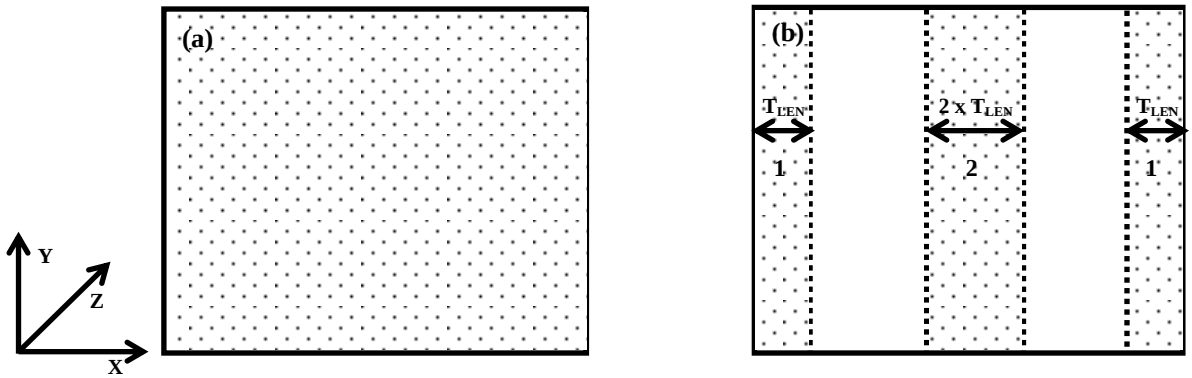

Figure 1: Thermostatting Scheme - Full Thermostatting (a) and Partial Thermostatting (b). Shaded area represents thermostatted regions. Particles of the unshaded regions are governed by the usual Hamilton's equations of motion.

Figure 1 represents the thermostatting scheme for both the full as well partial thermostatting case. T_{LEN} represents the proportion of the system under the influence of the thermostatting scheme. This kind of arrangement ensures that periodic boundary conditions can be implemented without breaking symmetry. The PB equations of motion, augmented with a switching function, for this kind of arrangement can be written as:

$$\begin{aligned}
\dot{r}_i &= \frac{p_i}{m_i} - \xi \frac{\partial \phi}{\partial r_i} S(r_i) \\
\dot{p}_i &= -\frac{\partial \phi}{\partial r_i} - \eta\, p_i S(r_i) \\
\dot{\xi} &= \frac{1}{Q_\xi} \sum_{i=1}^{3N} \left(\left(\frac{\partial \phi}{\partial r_i} \right)^2 - k_B T_0 \frac{\partial^2 \phi}{\partial r_i^2} \right) S(r_i) \\
\dot{\eta} &= \frac{1}{Q_\eta} \sum_{i=1}^{3N} \left(\frac{p_i^2}{m_i} - k_B T_0 \right) S(r_i)
\end{aligned} \tag{5}$$

The switch $S(r_i)$ is an indicator function taking up a value of 1 when the i^{th} particle is in the thermostatted region. It is interesting to note that (5) reduces to the usual Hamilton's equations for the particles that are not under the influence of any thermostats (i.e. in the unshaded region). The NH and BT EOM are generalized similarly. A thermal conduction process is simulated by

keeping the regions 1 and 2 at different temperatures, thereby requiring four thermostat variables (two for hot and two for cold temperatures) and two switching functions. The selection of thermostat masses is done in a manner that the mean-squared feedback of the kinetic variables is roughly two orders of magnitude larger than the mean-squared feedback of the configurational variables. This is done to ensure that the configurational variables relax slowly than the kinetic variables.

3. NUMERICAL SIMULATIONS AND RESULTS

The numerical simulations have been designed in such a manner that they are able to capture the equivalence/difference between the different thermostats. Extensive equilibrium simulations have been performed to show that the radial distribution function due to the different thermostats is identical. The difference between the different thermostats is captured using nonequilibrium simulations. To be more specific, we look at the (i) radial distribution function, and (ii) consistency in temperature profile for the problem of nonequilibrium thermal conduction for varied system size and temperature difference.

For all the cases, we have chosen a number density of 0.725 (a highly dense system). The system domain is a cubic box with periodic boundary conditions in all the directions. Initial particle positions are sampled from a uniform distribution and their velocities from the Maxwell-Boltzmann distribution. Pair wise interaction (ϕ_{ij}) of Lennard-Jones type with a cut-off radius of 2.5 is assumed:

$$\phi_{ij} = 4\left[\left(\frac{1}{r_{ij}}\right)^{12} - \left(\frac{1}{r_{ij}}\right)^{6}\right] \quad r_{ij} \le 2.5 \tag{6}$$

Equilibration is achieved in two steps: first a conjugate gradient based energy minimization followed by 50,000 MD steps. The integration in MD is performed using the Gear Predictor-Corrector algorithm [37] for the PB and NH thermostats, and the Velocity-Verlet algorithm for BT thermostat, the time step being 0.001fs for both. T_{LEN} was assumed to be 10% of the simulation box length.

i. Equilibrium Simulations:

We look at the radial distribution function for the three thermostats. At equilibrium, radial distribution function contributes towards the entropy in totality. Thus, if the different thermostats yield the same radial distribution function, it would imply that all these thermostats result in

identical thermodynamic properties at equilibrium. This is because entropy is directly related to different thermodynamic quantities through exact mathematical expressions. In fact, one can relate radial distribution function to properties like structure factor, potential of mean force, potential energy, pressure etc. The system temperature was kept at 2.0. Figure 2 shows the RDF for the different thermostats as well as system size (at fixed number density).

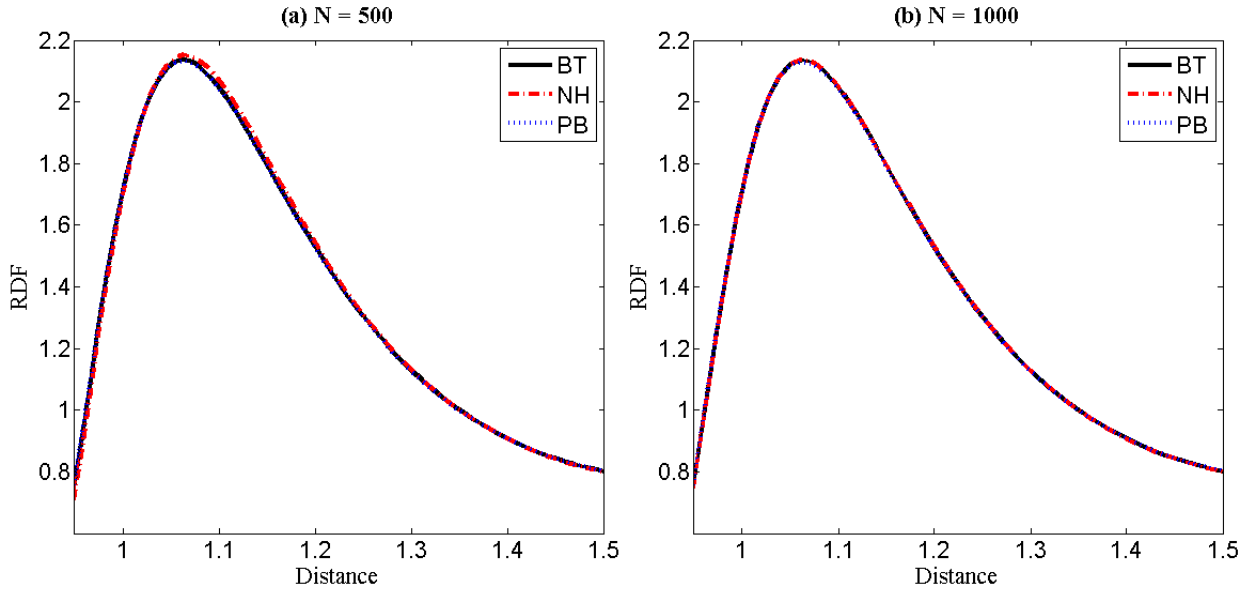

Figure 2: Radial Distribution Function for the system in equilibrium using the three thermostats. The RDFs due to the three thermostats overlap each other, suggesting that in equilibrium dynamical properties are not thermostat dependent.

It can be clearly observed that the RDFs due to the different thermostats at equilibrium overlap. The equality of RDFs, and consequently the macroscopic properties of the system, indicate that the different thermostats perform comparably well in equilibrium. Choice of thermostats, therefore, for studying equilibrium properties is irrelevant.

ii. Nonequilibrium Simulations:

The difference between the different thermostats can be observed clearly using nonequilibrium simulations. For these cases, the PB thermostat has been shown to be the only thermostat that is able to generate a consistent temperature profile. In the present study, we simulate a thermal conduction process by keeping the regions 1 and 2 of Figure 1(b) at different temperatures. In this study, we check if the consistency in temperature profile is still maintained at higher temperature difference.

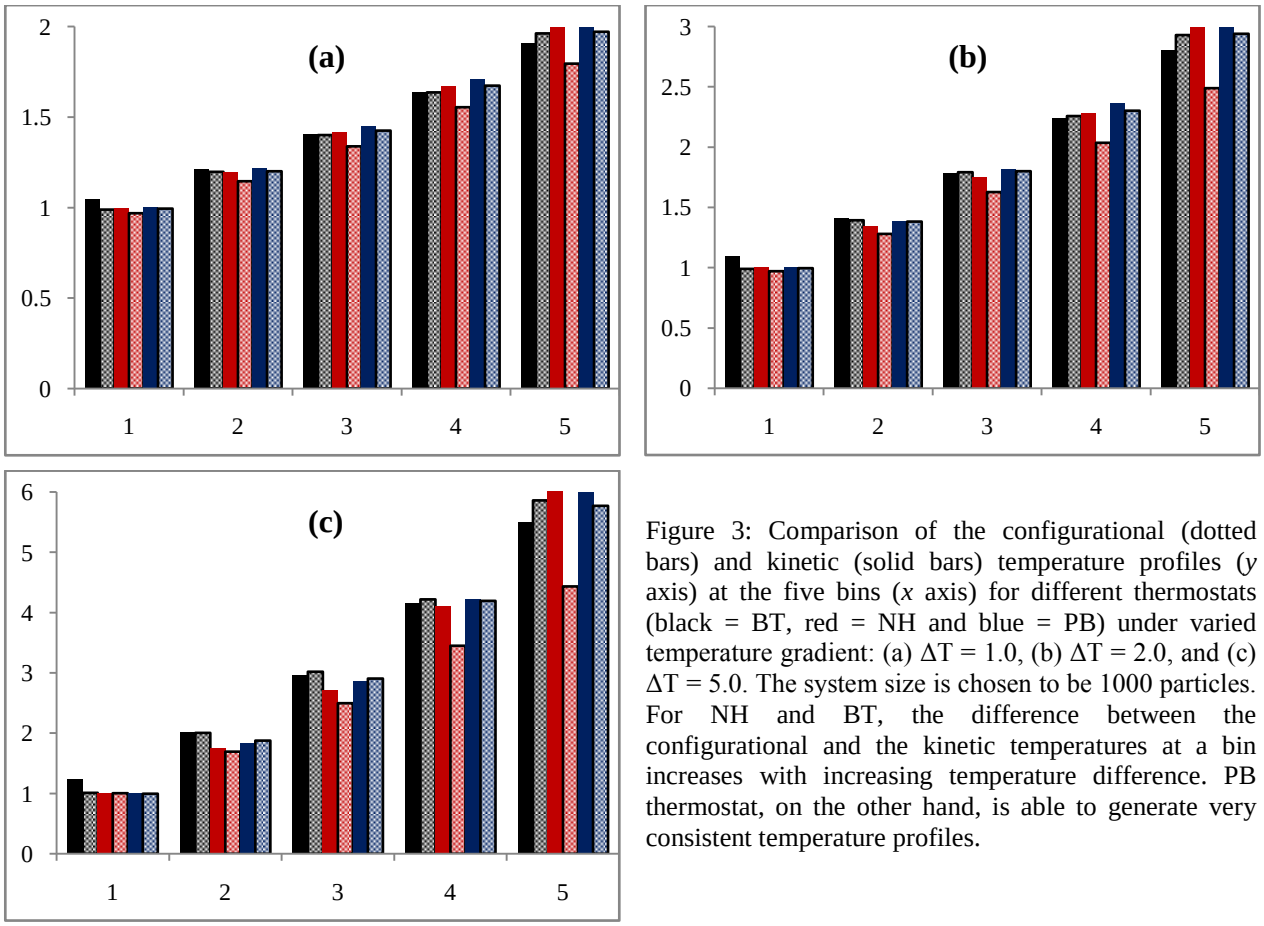

Figure 3: Comparison of the configurational (dotted bars) and kinetic (solid bars) temperature profiles (*y* axis) at the five bins (*x* axis) for different thermostats (black = BT, red = NH and blue = PB) under varied temperature gradient: (a) $\Delta T = 1.0$, (b) $\Delta T = 2.0$, and (c) $\Delta T = 5.0$. The system size is chosen to be 1000 particles. For NH and BT, the difference between the configurational and the kinetic temperatures at a bin increases with increasing temperature difference. PB thermostat, on the other hand, is able to generate very consistent temperature profiles.

Figure 3 shows the effect of increasing the temperature difference (ΔT) on the temperature profiles for a system comprising of 1000 particles. Due to the symmetry, we only study half of the system, which is divided into 5 spatial bins of equal spacing. It can be observed clearly that with increasing temperature difference, the difference between the kinetic and configurational temperatures due to NH and BT thermostats increases. In fact in some of the cases (see Figure 3(c)), the BT thermostat is not even able to keep the temperature of the higher end at the desired value. The PB thermostat, on the other hand, is able to generate a relatively consistent temperature profile even for large temperature difference, highlighting its superiority over other thermostats. We observed a similar behaviour when the system size was increased to 2000 particles. The PB thermostat still performed the best amongst the three thermostats. From Figure 3, it is clear that the properties due to the three thermostats, despite being identical in equilibrium, are not the same in nonequilibrium.

To emphasize the difference between the different thermostats, we will next show that the nonequilibrium RDFs due to the three thermostats are not the same. Although, RDFs in

nonequilibrium are not a sufficient metric to evaluate "nonequilibrium entropy", for the present purpose we deem it sufficient enough to highlight the qualitative differences of the dynamics due to the different thermostats.

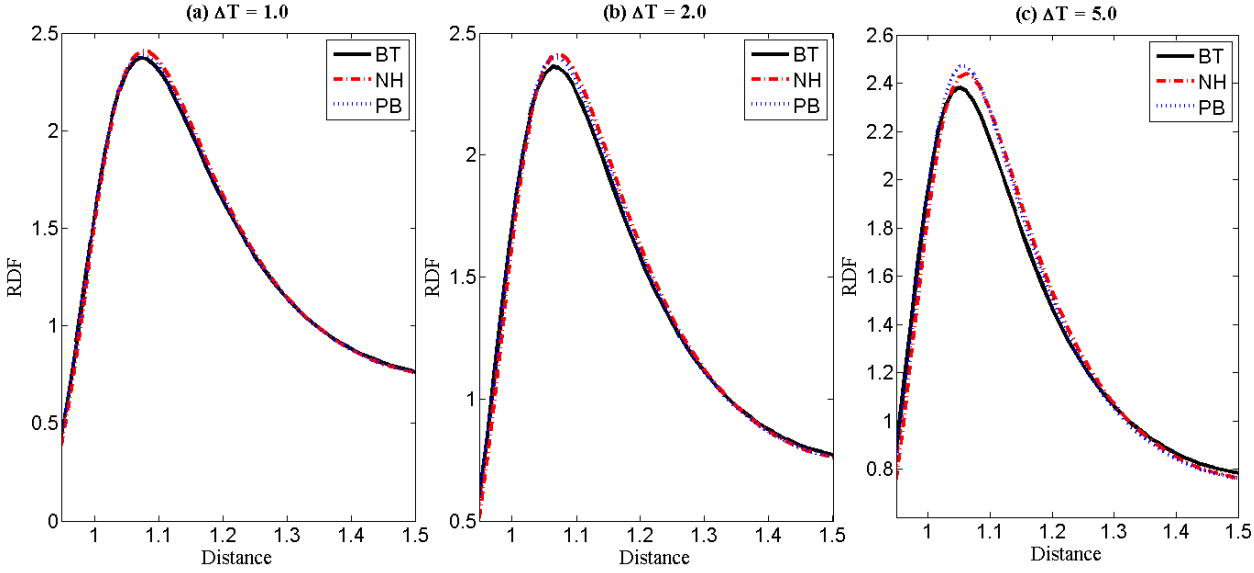

Figure 4: Radial distribution functions due to the three thermostats (black = BT, red = NH and blue = PB) for different temperature differences: (a) $\Delta T = 1.0$, (b) $\Delta T = 2.0$, and (c) $\Delta T = 5.0$. At low temperature differences, the RDFs due to the three thermostats are similar. However, as temperature difference increases, the difference between the RDFs due to the thermostats also increases. The system comprises of 1000 particles.

The RDFs due to the three thermostats are shown in Figure 4. It is interesting to see that at low temperature difference, the RDFs for all three thermostats *nearly* overlap. As the temperature difference increases, so does the disparity between the RDFs. A similar behaviour was observed by increasing the system size to 2000 particles. At this point, we would like to highlight that we do not have sufficient data / knowledge to comment upon which of the three RDFs is more accurate. However, when combined with the results regarding consistency of temperature profiles, our judgement is that the PB thermostat is likely to provide more accurate results.

4. CONCLUSIONS

In this work, we highlighted the relative advantages of using the Patra-Bhattacharya (PB) thermostat, that constrains both the kinetic as well as the configurational temperatures, over other thermostats that constrain either the kinetic (the Nosé-Hoover thermostat) or the configurational (the Braga-Travis thermostat) temperature. To demonstrate these advantages, we perform nonequilibrium molecular dynamics simulations by bringing the system in contact with two thermal reservoirs kept at different temperatures. The resulting temperature difference drives a heat flow in the system. Only the systems under the influence of PB thermostats have a

consistent temperature profile. For both the NH as well as the BT thermostatted systems, the difference between the kinetic and the configurational temperatures is substantially large. Further, this difference increases upon increasing the imposed temperature difference.

The difference in the temperature profiles for the different thermostats in the nonequilibrium scenario suggests strong thermostat dependent dynamical properties of the system, as has been observed previously. On the other hand, equilibrium simulations using these thermostats suggest that equilibrium properties are thermostat independent.

To concretize our argument we calculated the nonequilibrium radial distribution functions (RDFs) due to the three thermostats. RDF is an important parameter that can be closely connected to several physical and thermodynamic variables. Our results suggest that at low temperature difference, like in equilibrium, the RDFs due to the different thermostats are nearly the same. However, at larger temperature differences, the RDFs show significant deviation from each other.

To conclude, in this work, we have shown (i) the different thermostats yield similar dynamical properties in equilibrium, (ii) in nonequilibrium cases thermostat dependent dynamical properties can be observed, and (iii) the Patra-Bhattacharya thermostat is able to generate relatively more consistent temperature profiles even under large temperature difference, suggesting its superiority over the other thermostats.

5. REFERENCES

1. Jones, A. and B. Leimkuhler, *Adaptive stochastic methods for sampling driven molecular systems.* The Journal of Chemical Physics, 2011. **135**(8): p. -.
2. Yao, Z., et al., *Thermal conduction of carbon nanotubes using molecular dynamics.* Physical Review B, 2005. **71**(8): p. 085417.
3. Dimastrogiovanni, D., et al., *molecular dynamics simulation of self-diffusion coefficient and its relation with temperature using simple lennard-jones potential.* Heat Transfer—Asian Research, 2008.
4. Evans, D.J., et al., *Nonequilibrium molecular dynamics via Gauss's principle of least constraint.* Physical Review A, 1983. **28**(2): p. 1016-1021.
5. Hoover, W.G., et al., *Lennard-Jones triple-point bulk and shear viscosities. Green-Kubo theory, Hamiltonian mechanics, and nonequilibrium molecular dynamics.* Physical Review A, 1980. **22**(4): p. 1690-1697.
6. Hoover, W.G., A.J.C. Ladd, and B. Moran, *High-Strain-Rate Plastic Flow Studied via Nonequilibrium Molecular Dynamics.* Physical Review Letters, 1982. **48**(26): p. 1818-1820.
7. Evans, D.J., *Computer ''experiment'' for nonlinear thermodynamics of Couette flow.* The Journal of Chemical Physics, 1983. **78**(6): p. 3297-3302.
8. Woodcock, L.V., *Isothermal molecular dynamics calculations for liquid salts.* Chemical Physics Letters, 1971. **10**(3): p. 257-261.
9. Andersen, H.C., *Molecular dynamics simulations at constant pressure and/or temperature.* The Journal of Chemical Physics, 1980. **72**(4): p. 2384-2393.
10. Grest, G.S. and K. Kremer, *Molecular dynamics simulation for polymers in the presence of a heat bath.* Physical Review A, 1986. **33**(5): p. 3628-3631.

11. Schneider, T. and E. Stoll, *Molecular-dynamics study of a three-dimensional one-component model for distortive phase transitions.* Physical Review B, 1978. **17**(3): p. 1302-1322.
12. Nose, S., *A unified formulation of the constant temperature molecular dynamics methods.* The Journal of Chemical Physics, 1984. **81**(1): p. 511-519.
13. Hoover, W.G., *Canonical dynamics: Equilibrium phase-space distributions.* Physical Review A, 1985. **31**(3): p. 1695-1697.
14. Martyna, G.J., M.L. Klein, and M. Tuckerman, *Nos[e-acute]--Hoover chains: The canonical ensemble via continuous dynamics.* The Journal of Chemical Physics, 1992. **97**(4): p. 2635-2643.
15. Hamilton, I.P., *Modified Nosé-Hoover equation for a one-dimensional oscillator: Enforcement of the virial theorem.* Physical Review A, 1990. **42**(12): p. 7467-7470.
16. Winkler, R.G., *Extended-phase-space isothermal molecular dynamics: Canonical harmonic oscillator.* Physical Review A, 1992. **45**(4): p. 2250-2255.
17. Hoover, W.G. and B.L. Holian, *Kinetic moments method for the canonical ensemble distribution.* Physics Letters A, 1996. **211**(5): p. 253-257.
18. Bond, S.D., B.J. Leimkuhler, and B.B. Laird, *The Nosé–Poincaré Method for Constant Temperature Molecular Dynamics.* Journal of Computational Physics, 1999. **151**(1): p. 114-134.
19. Patra, P.K. and B. Bhattacharya, *A deterministic thermostat for controlling temperature using all degrees of freedom.* The Journal of Chemical Physics, 2014. **140**(6): p. -.
20. Watanabe, H. and H. Kobayashi, *Ergodicity of a thermostat family of the Nosé-Hoover type.* Physical Review E, 2007. **75**(4): p. 040102.
21. Posch, H.A., W.G. Hoover, and F.J. Vesely, *Canonical dynamics of the Nosé oscillator: Stability, order, and chaos.* Physical Review A, 1986. **33**(6): p. 4253-4265.
22. Samoletov, A.A., C.P. Dettmann, and M.A.J. Chaplain, *Notes on configurational thermostat schemes.* The Journal of Chemical Physics, 2010. **132**(24): p. 246101-2.
23. Legoll, F., M. Luskin, and R. Moeckel, *Non-Ergodicity of the Nosé–Hoover Thermostatted Harmonic Oscillator.* Archive for Rational Mechanics and Analysis, 2007. **184**(3): p. 449-463.
24. Watanabe, H. and H. Kobayashi, *Ergodicity of the Nosé–Hoover method.* 2007.
25. Patra, P.K. and B. Bhattacharya, *Nonergodicity of the Nose-Hoover chain thermostat in computationally achievable time.* Physical Review E, 2014. **90**(4): p. 043304.
26. Rugh, H.H., *Dynamical Approach to Temperature.* Physical Review Letters, 1997. **78**(5): p. 772-774.
27. Butler, B.D., et al., *Configurational temperature: Verification of Monte Carlo simulations.* The Journal of Chemical Physics, 1998. **109**(16): p. 6519-6522.
28. Jepps, O.G., G. Ayton, and D.J. Evans, *Microscopic expressions for the thermodynamic temperature.* Physical Review E, 2000. **62**(4): p. 4757-4763.
29. Casas-Vázquez, J. and D. Jou, *Temperature in non-equilibrium states: a review of open problems and current proposals.* Reports on Progress in Physics, 2003. **66**(11): p. 1937.
30. Evans, D.J. and G. Morriss, *Statistical Mechanics of Nonequilibrium Liquids*. 2 edition ed. 2008: Cambridge University Press.
31. Braga, C. and K.P. Travis, *A configurational temperature Nos[e-acute]-Hoover thermostat.* The Journal of Chemical Physics, 2005. **123**(13): p. 134101-15.
32. Basconi, J.E. and M.R. Shirts, *Effects of Temperature Control Algorithms on Transport Properties and Kinetics in Molecular Dynamics Simulations.* Journal of Chemical Theory and Computation, 2013. **9**(7): p. 2887-2899.
33. Hoover, W.G. and C.G. Hoover, *Hamiltonian thermostats fail to promote heat flow.* Communications in Nonlinear Science and Numerical Simulation, 2013. **18**(12): p. 3365-3372.
34. Hoover, W.G., *Computational Statistical Mechanics*. 1991, Amsterdam: Elsevier.
35. Cho, K. and J.D. Joannopoulos, *Ergodicity and dynamical properties of constant-temperature molecular dynamics.* Physical Review A, 1992. **45**(10): p. 7089-7097.
36. Tobias, D.J., G.J. Martyna, and M.L. Klein, *Molecular dynamics simulations of a protein in the canonical ensemble.* The Journal of Physical Chemistry, 1993. **97**(49): p. 12959-12966.
37. Sadus, R.J., *Molecular Simulations of Fluid: Theory, Algorithms and Object Oriented*. 2002: Elsevier.